Nigerian Journal of Physics (NJP)
ISSN online: 3027-0936
ISSN print: 1595-0611
DOI: https://doi.org/10.62292/njp.v33i2.2024.214
Volume 33(2), June 2024

Effect of Al Dope with ZnO Electron Transport Layer in Perovskite Solar Cells Using SCAPs 1-D Simulation

***[1,2]Yusuf, A. S., [3]Ramalan, A. M., [1]Abubakar, A. A., [1]Mohammed, I. K., [1]Ibrahim, S. O., [4]Adamu, F. E., [1]Ahmadu, U. and [1]Isah, K. U.**

[1]Department of Physics, Federal University of Technology, P.M.B 65, Minna, Nigeria.
[2]Department of Physics and Astronomy, Auckland University of Technology, New Zealand.
[3]Department of Physics, University of Abuja, P.M. B 117, Abuja, Nigeria.
[4]Department of Physics, Ibrahim Badamasi Babangida University, P.M.B 74, Lapai Nigeria.

*Corresponding author's email: ayusuf@futminna.edu.ng

Keywords:
ZnO,
Al,
Electron transport layer,
Perovskite solar cell,
Power conversion efficiency,
SCAPS 1D.

ABSTRACT

Perovskite solar cells have shown exceptional performance and significant advancements in solar cell efficiency. For perovskite solar cells to conduct electrons and generate current, one of the key components is the substance known as the electron transport layer (ETL). Using the SCAPS 1D modelling program, ZnO: Al was used in this instance as the ETL material in a perovskite solar cell. Because of its interaction with the perovskite material, the ZnO: Al ETL demonstrated high cell efficiency. The performance of the ZnO: Al-doped-based solar cell achieved a PCE as high as 23.5%. In the meanwhile, the greatest cell performance in terms of enhancing the charge transport mechanism and raising cell efficiency was shown by perovskite solar cells doping the ETL with Al and having the right layer thickness. Thus, throughout the manufacturing process, the parameters used in this study may serve as a guide.

INTRODUCTION

Global population growth is increasing annually, leading to a rise in the need for energy. Furthermore, the increasing use of technology in everyday life increases the amount of energy used. Since fossil fuels like coal, oil, and natural gas are not renewable, their supply of conventional energy will eventually run out. One of the most popular renewable energy sources for producing electricity is solar energy. If sunlight reaches the earth, this source has no limits. Numerous solar cell varieties, including organic, thin-film, and silicon-based solar cells, have been created and brought to market (N. Noorasid et al., 2022; N. S. Noorasid et al., 2022). Researchers have recently been interested in perovskite solar cells (PSC) due to their remarkable power conversion efficiency (PCE) growth within a short period. An organic-inorganic perovskite layer, a hole transport layer (HTL), and an electron transport layer (ETL) make up a PSC's primary layers (Nizamuddin et al., 2020). By guaranteeing quick charge transfer from the perovskite active layer to the electrode without being hampered by charge recombination, ETL material plays a significant role in enhancing cell performance (Ahn et al., 2015).

A PSC with a PCE as high as 25.5% was created in 2020 by the Ulsan National Institute of Science and Technology (UNIST) in South Korea. The fluorination approach was used to chemically improve the HTL layer of Spiro-OMETAD (Jeong et al., 2020). Oxford PV, a prominent player in the perovskite solar cell industry, recently announced that the highest PCE value ever recorded to date 29.49 % had been reached (Vogt et al., 2022). Nonetheless, TiO_2 is often used as the ETL material in these traditional PSCs. TiO_2 is a good hole-blocker at the perovskite interface and provides excellent photostability and a suitable band gap for effective electron transport from the perovskite layer (Suhaimy et al., 2020). However, annealing at high temperatures (over 500°C) is necessary to develop a high-quality TiO_2 ETL, which compromises the viability of flexible PSCs (Alias et al., 2022). An alternate ETL material called ZnO has been suggested; it offers a low thermal budget production procedure, about the same band gap, and greater electron mobility when compared to a TiO_2 ETL (Alias et al., 2022). The work function (WF) of the ETL and conductivity are two critical elements that affect the electron extraction capabilities of the ETL in a PSC. By adding a little quantity of impurity (Alias et al., 2022) of Al

extrinsically, ZnO electrical conductivity may be enhanced. Zn^{2+} has a greater ion radius (0.74 Å) than Al^{3+} (0.54 Å), hence at the lattice site, a little quantity of Al^{3+} may inadvertently replace Zn^{2+}. Then, it may function as an extra dopant, improving the ZnO ETLs conductivity while preserving its outstanding transparency in the visible light spectrum (Tseng et al., 2016).

Here, the SCAPS 1D simulation program was used to examine Al-doped ZnO as an ETL material in a PSC. To find the ideal device structure, other important factors were also changed, including layer thickness, operating temperature, doping concentration, and defect density (Ahmed et al., 2021). It was discovered that a small quantity of aluminum enhanced the ZnO ETL's electrical conductivity. When compared to Al-doped with ZnO, a standard ZnO ETL of PSC generated a comparatively lower PCE because of the organic cation ($CH_3NH_3\neg^+$) of perovskite interacting with the ZnO (Bhoomanee et al., 2019). The greatest PCE was achieved as high as 23.5 %. Numerous earlier investigations (Rahman et al., 2012; Tseng et al., 2016) found a limit to the solubility of Al^{3+} substitution in ZnO to confirm this conclusion.

Perovskite Solar Cell Simulation

In this work, the electrical properties of PSC were investigated using the SCAPS 1D simulation program. The University of Gent in Belgium's Department of Electron and Information Systems (ELIS) created and released the simulation software (Burgelman et al., 2007). This program was first created for the thin film group's cell architectures. However, the capabilities of this program have been enhanced to the point that it can now be used with crystalline solar cells (Si and GaAs family), amorphous cells (a-Si and micromorphous Si), and the newly developed perovskite solar cells. The layer structure of the PSC used in the SCAPS simulation and the SCAPS-1D definition panel with layers names are shown in Figures 1 and 2, respectively. Using $CH_3NH_3PbI_3$ as the perovskite layer and Al doped-ZnO and Spiro-OMETAD as the HTL and ETL, respectively, the PSC was simulated. To optimize the Al doped-ZnO layer, this research examined and changed several critical factors, including layer thickness, doping concentration, operating temperature, and defect density. In addition, to achieve the ideal overall concentration, a little quantity of aluminum (Al) extrinsically doped into the ZnO layer with 2.5 mol %. Values of V_{OC} and J_{SC} changed because of combining different material properties into SCAPS for every part of the study; this had an impact on FF and PCE. Table 1 provides an explanation of the simulation's parameters as well as the foundation for the parameters used in this investigation.

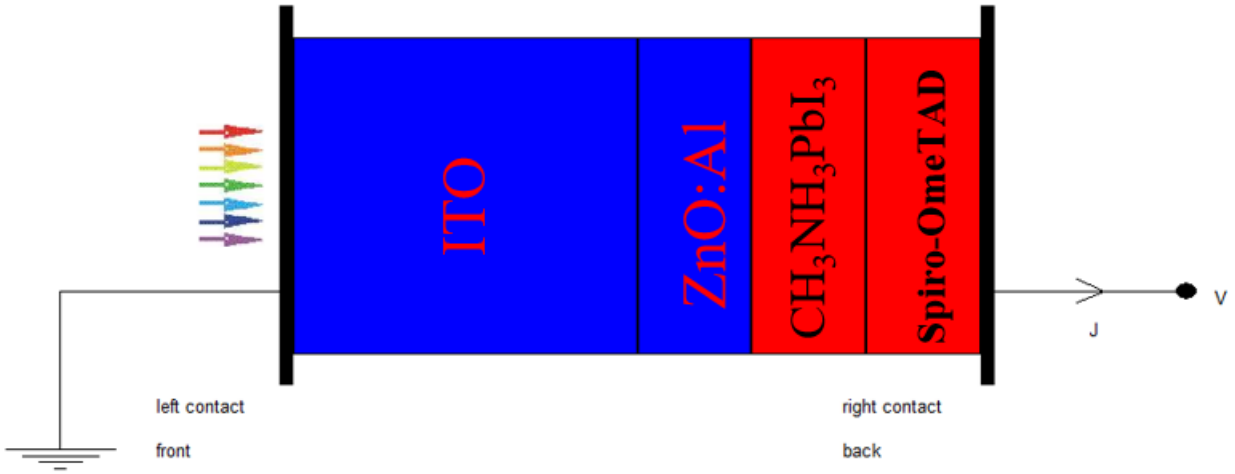

Figure 1: Perovskite solar cells layer architecture with SCAPS-1D

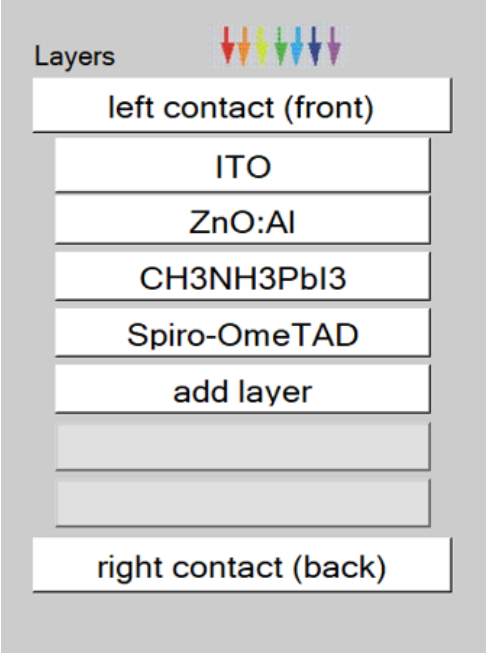

Figure 2: SCAPS-1D definition panel with layers name

Table 1: List of parameter values of the device interface

Parameters	**ITO (Du et al., 2016; Liu & Kelly, 2014)**	**$CH_3NH_3PbI_3$ (Aseena et al., 2021)**	**Spiro-OmeTAD (Bansal & Aryal, 2016)**	**Concentrations ZnO:Al (mol %) 2.5 (Rahman et al., 2012)**
Thickness (nm)	300	100	100	100
Band gap (eV)	3.6	1.51	2.9	3.25
Electron affinity (eV)	4.2	4.0	2.2	4
Dielectric permittivity	10	6.6	3	9
CB effective density of states (cm^{-3})	2×10^{18}	$1 \times 2 \times 10^{19}$	$2 \times 2 \times 10^{18}$	$2 \times 3 \times 10^{18}$
VB effective density of states (cm^{-3})	$1 \times 8 \times 10^{19}$	$2 \times 9 \times 10^{18}$	$1 \times 8 \times 10^{18}$	$1 \times 8 \times 10^{18}$
Thermal velocity of electrons (cm/s)	10^7	10^7	10^7	10^7
Thermal velocity of holes (cm/s)	10^7	10^7	10^7	10^7
Electron mobility (cm^2/Vs)	50	2.7	10^{-4}	300
Hole mobility (cm^2/Vs)	75	1.8	10^{-4}	25
Shallow donor density N_D (cm^{-3})	10^{19}	0	0	$7 \times 2 \times 10^{19}$
Shallow acceptor density N_A (cm^{-3})	0	$1 \times 3 \times 10^{16}$	10^{18}	0
Defect density N_t (cm^{-3})	10^{15}	4×10^{13}	10^{15}	10^{15}

Device architecture

The structure employed in this simulation is the n-i-p planar structure which is the most basic and common PSC Cell Structure (Khattak et al., 2020; Shen et al., 2016). It consists of 4 main layers as shown in Figure. 1.The first layer is the Indium-doped tin oxide (ITO) glass. It not only acts as the base for the cell structure to be fabricated upon but also acts as the negative electrode (cathode). On top of the ITO is the ETL. ETL collects the negative charged ions from the cell. The absorber layer made of perovskite material is placed on top of the ETL. This is where the charge carriers are produced when the structure is exposed to light. On top of the absorber layer is the hole transport layer (HTL) which collects the positive charged ions from the absorber. The final layer is the positive electrode (anode) which collects the holes produced from the cell. In this study, the Methylammonium lead Iodide ($CH_3NH_3PbI_3$) was used as the perovskite absorber material due to its better stability than Sn based perovskite solar cell. The n-type tin oxide (ZnO:Al) is used as the ETL and p-type Spiro-OMeTAD is used as

hole transport layer. Whereas silver (Ag) is used as anode material. The final structure of the PSC model is (FTO/ZnO:Al/ $CH_3NH_3PbI_3$/Spiro-OmeTAD/Ag).

Device modelling

The complete PSC structure of (FTO/ZnO:Al/ $CH_3NH_3PbI_3$/Spiro-OmeTAD/Ag) is modelled layer by layer on SCAPS. The required material parameters for all the layers are obtained from multiple experimental and theoretical published data (Bansal & Aryal, 2016; Du et al., 2016; Karthick et al., 2020; Liu & Kelly, 2014; Stamate, 2003; Stanic et al., 2021).

RESULTS AND DISCUSSION

Influence of working temperature

To see how much the operating temperature affects cell performance in the actual world, an operating temperature between 300k and 350k was simulated. High temperatures will react and have an impact on several characteristics in semiconductor devices, including material band gaps, carrier concentration, and electron and hole mobility (noorasid et al., 2021). Consequently, there is less electron flow, which has an impact on the cell's efficiency. It is evident that every device had a consistent declining trend as the temperature rose. At lower temperatures, all devices showed a comparatively smaller gradient. This is most likely because the bandgap narrowing process is slowed down. The bandgap often narrows as temperature rises, which most likely encourages charge carrier recombination between the valence band and the conduction band. Furthermore, a rise in defect density within the layers, which affects deformation stress, might potentially be the cause of the decline in cell efficiency (slami et al., 2020).

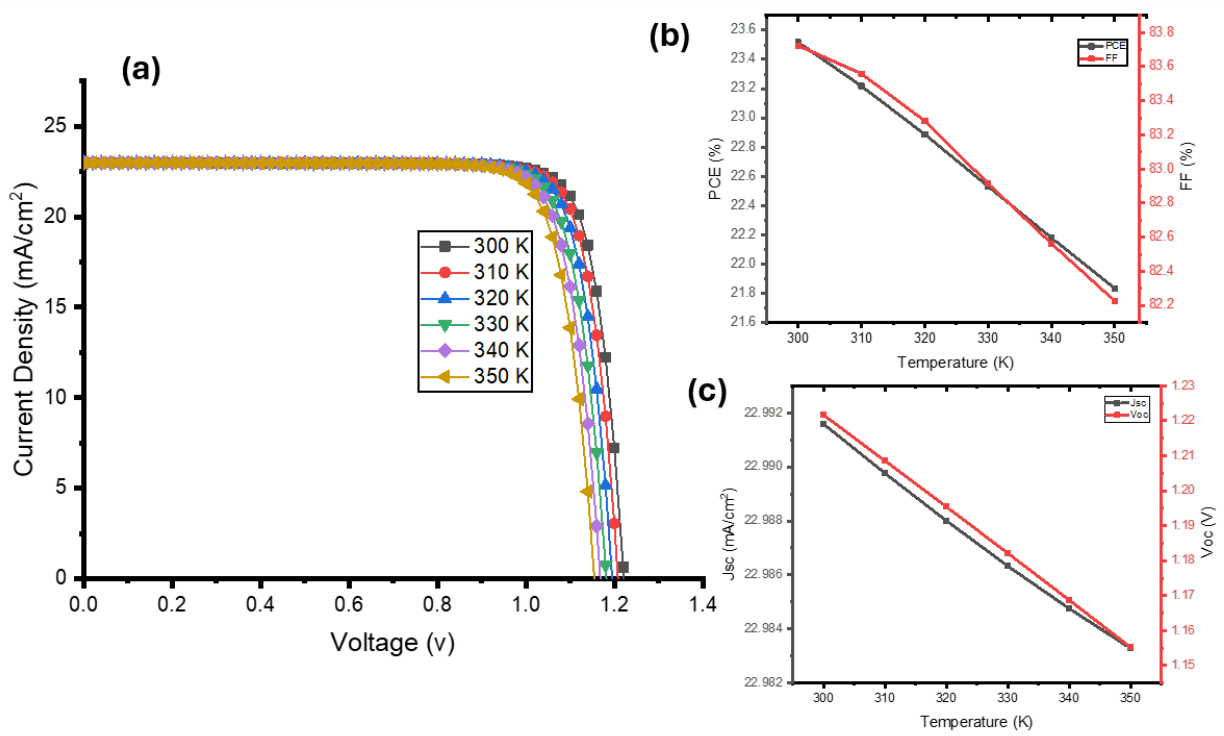

Figure 3: (a) J-V curve with varied working temperature, (b) PCE and FF and (c) J_{SC} and V_{OC} with respect to varied working temperature

Influence of ZnO:Al thickness

There was a variation in the thickness of (ZnO:Al) ETL between 100 and 600 nm. Given the capabilities of cell manufacture, the range chosen was adequate. Every device's PCE values peaked at a thickness of 100 nm. Furthermore, as seen in Figure 4, the maximum PCE value, or up to 23.5 %, was found at the latter thickness and throughout the whole range under investigation. At greater thicknesses, the ZnO:Al layers had the lowest peak value. When ETL thickness increased, the PCE value dropped. Because the charge must diffuse over greater distances, increasing the thickness of ETL reduces PCE and raises the possibility of recombination. But when thickness increases, its effectiveness drops down at a given pace, most likely because of more recombination (Anwar et al., 2017; Correa-Baena et al., 2016).

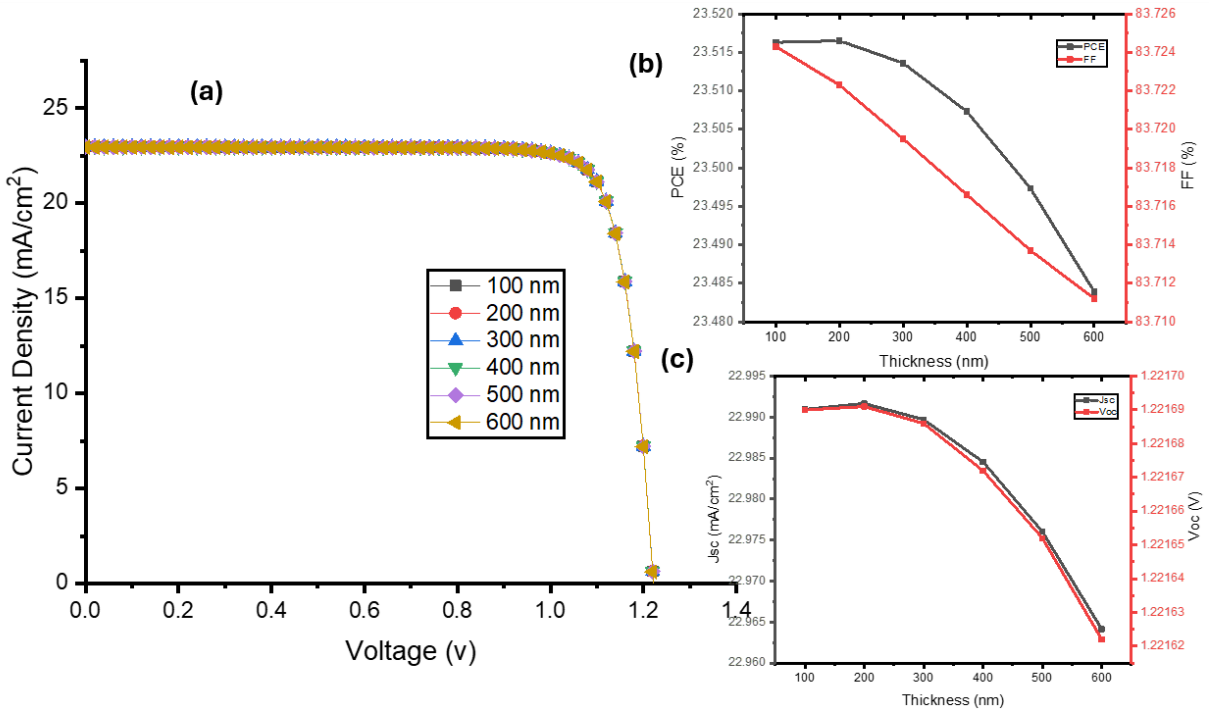

Figure 4: (a) J-V curve with varied ETL thickness, (b) PCE and FF and (c) J_{SC} and V_{OC} with respect to varied ETL thickness

Influence of ZnO:Al doping concentration

ETL's doping concentration is essential for speeding up electron flow and, therefore, current generation. The charge carrier conductivity is increased when n-type Al dopant is inserted into the ZnO ETL to replace the Zn^{2+}. This successfully suppresses the ETL/perovskite interface defects. The Al dopants also introduce a donor level at 120 meV below the conduction band, which is promoted to the proper band alignment, and raise the concentrations of free carriers (Mahmood et al., 2022). An ideal value with the least amount of doping will provide a solar cell with excellent performance. Here, each device's doping level ranged from 10^{13} to 10^{18} cm^{-3}. To provide for a fair comparison, the other parameters' layer temperature and thickness were fixed. Figure 5 illustrates how, for all devices, cell efficiency rose with doping concentration up to 1×10^{18} cm^{-3} before plateauing. At high doping concentration, it was found that the device with 1×10^{18} cm^{-3} performed the best. The higher electric field within the cell is what causes the improvement in cell efficiency. The performance of the solar cell will be enhanced by the increased electric field since it will further intensify the charge carrier separation activity (Hao et al., 2021).

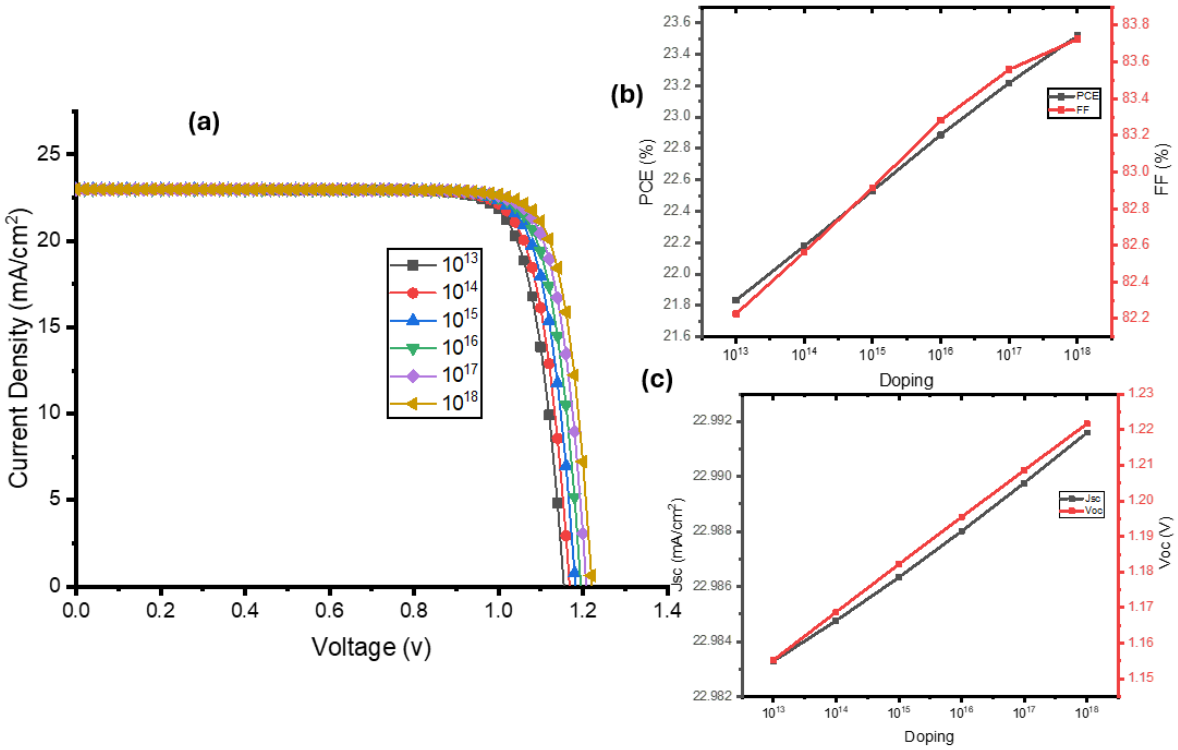

Figure 5: (a) J-V curve with varied ETL doping, (b) PCE and FF and (c) J_{SC} and V_{OC} with respect to varied ETL doping

CONCLUSION

This study outlined the most effective method for doping ZnO ETL with aluminum to boost PSC efficiency. To attain ideal cell characteristics, PSCs were simulated with the use of the SCAP 1D simulation program. A thorough investigation and connection between the layer thickness, doping, and operating temperature of an Al-doped ZnO ETL were carried out. Up to 23.5% of simulated PSC cell efficiencies were achieved. ZnO ETL doped with Al, 100 nm-thick layers. Previous publications state that thickness as thin as 10 nm ZnO ETL is necessary to produce PCEs over 15 %, necessitating the work of complex and expensive control equipment. Thus, our study has shown that it is possible to increase PSC performance while maintaining cost effectiveness by adjusting and fine-tuning the major parameters of the Al-doped ZnO ETL. Furthermore, the cell production procedure may be guided by these factors.

ACKNOWLEDGEMENT

We express our heartfelt gratitude to Dr. Marc Burgelman of the University of Gent in Belgium's Department of Electron and Information Systems (ELIS) who created and released the simulation software for free.

REFERENCES

Ahmed, S., Jannat, F., Khan, M. A. K., & Alim, M. A. (2021). Numerical development of eco-friendly Cs_2TiBr_6 based perovskite solar cell with all-inorganic charge transport materials via SCAPS-1D. *Optik*, *225*, 165765.

Ahn, N., Son, D.-Y., Jang, I.-H., Kang, S. M., Choi, M., & Park, N.-G. (2015). Highly reproducible perovskite solar cells with average efficiency of 18.3% and best efficiency of 19.7% fabricated via Lewis base adduct of lead (II) iodide. *Journal of the American Chemical Society*, *137*(27), 8696-8699.

Alias, N., Arith, F., Mustafa, A., Ismail, M., Chachuli, S., & Shah, A. (2022). Compatibility of Al-doped ZnO electron transport layer with various HTLs and absorbers in perovskite solar cells. *Applied Optics*, *61*(15), 4535-4542.

Anwar, F., Mahbub, R., Satter, S. S., & Ullah, S. M. (2017). Effect of different HTM layers and electrical parameters on ZnO nanorod-based lead-free perovskite solar cell for high-efficiency performance. *International Journal of Photoenergy*, *2017*.

Aseena, S., Abraham, N., & Babu, V. S. (2021).

Optimization of layer thickness of ZnO based perovskite solar cells using SCAPS 1D. *Materials Today: Proceedings*, *43*, 3432-3437.

Bansal, S., & Aryal, P. (2016). Evaluation of new materials for electron and hole transport layers in perovskite-based solar cells through SCAPS-1D simulations. 2016 IEEE 43rd Photovoltaic Specialists Conference (PVSC),

Bhoomanee, C., Ruankhama, P., Choopun, S., Prathan, A., & Wongratanaphisan, D. (2019). Effect of al-doped ZnO for electron transporting layer in planar perovskite solar cells. *Materials Today: Proceedings*, *17*, 1259-1267.

Burgelman, M., Verschraegen, J., Minnaert, B., & Marlein, J. (2007). Numerical simulation of thin film solar cells: practical exercises with SCAPS. Proceedings of NUMOS (Int. Workshop on Numerical Modelling of Thin Film Solar Cells, Gent (B), Gent. 2007,

Correa-Baena, J.-P., Anaya, M., Lozano, G., Tress, W., Domanski, K., Saliba, M., Matsui, T., Jacobsson, T. J., Calvo, M. E., & Abate, A. (2016). Unbroken perovskite: interplay of morphology, electro-optical properties, and ionic movement. *Adv. Mater*, *28*(25), 5031-5037.

Du, H.-J., Wang, W.-C., & Zhu, J.-Z. (2016). Device simulation of lead-free $CH_3NH_3SnI_3$ perovskite solar cells with high efficiency. *Chinese Physics B*, *25*(10), 108802. https://doi.org/10.1088/1674-1056/25/10/108802

Hao, L., Li, T., Ma, X., Wu, J., Qiao, L., Wu, X., Hou, G., Pei, H., Wang, X., & Zhang, X. (2021). A tin-based perovskite solar cell with an inverted hole-free transport layer to achieve high energy conversion efficiency by SCAPS device simulation. *Optical and Quantum Electronics*, *53*, 1-17.

Jeong, M., Choi, I. W., Go, E. M., Cho, Y., Kim, M., Lee, B., Jeong, S., Jo, Y., Choi, H. W., & Lee, J. (2020). Stable perovskite solar cells with efficiency exceeding 24.8% and 0.3-V voltage loss. *Science*, *369*(6511), 1615-1620.

Karthick, S., Velumani, S., & Bouclé, J. (2020). Experimental and SCAPS simulated formamidinium perovskite solar cells: A comparison of device performance. *Solar Energy*, *205*, 349-357. https://doi.org/10.1016/j.solener.2020.05.041

Khattak, Y. H., Baig, F., Shuja, A., Beg, S., & Soucase, B. M. (2020). Numerical analysis guidelines for the design of efficient novel nip structures for perovskite solar cell. *Solar Energy*, *207*, 579-591.

Liu, D., & Kelly, T. L. (2014). Perovskite solar cells with a planar heterojunction structure prepared using room-temperature solution processing techniques. *Nature Photonics*, *8*(2), 133-138. https://doi.org/https://doi.org/10.1038/nphoton.2013.342

Mahmood, A., Munir, T., Fakhar-e-Alam, M., Atif, M., Shahzad, K., Alimgeer, K., Gia, T. N., Ahmad, H., & Ahmad, S. (2022). Analyses of structural and electrical properties of aluminium doped ZnO-NPs by experimental and mathematical approaches. *Journal of King Saud University-Science*, *34*(2), 101796.

Nizamuddin, A., Arith, F., Rong, J., Zaimi, M., Rahimi, A. S., & Saat, S. (2020). Investigation of copper (I) thiocyanate (CuSCN) as a hole transporting layer for perovskite solar cells application. *Journal of Advanced Research in Fluid Mechanics and Thermal Sciences*, *78*(2), 153-159.

Noorasid, N., Arith, F., Mustafa, A., Azam, M., Mahalingam, S., Chelvanathan, P., & Amin, N. (2022). Current advancement of flexible dye sensitized solar cell: A review. *Optik*, *254*, 168089.

Noorasid, N. S., Arith, F., Firhat, A. Y., Mustafa, A. N., & Shah, A. S. M. (2022). SCAPS Numerical Analysis of Solid-State Dye-Sensitized Solar Cell Utilizing Copper (I) Iodide as Hole Transport Layer. *Engineering Journal*, *26*(2), 1-10.

Noorasid, N. S., Arith, F., Mustafa, A. N., Azam, M. A., Suhaimy, S. H. M., & AL-ANI, O. A. (2021). Effect of Low Temperature Annealing on Anatase TiO_2 Layer as Photoanode for Dye-Sensitized Solar Cell. *Przeglad Elektrotechniczny*, *97*(10).

Rahman, M. M., Khan, M., Islam, M. R., Halim, M., Shahjahan, M., Hakim, M., Saha, D. K., & Khan, J. U. (2012). Effect of Al doping on structural, electrical, optical and photoluminescence properties of nano-structural ZnO thin films. *Journal of Materials Science & Technology*, *28*(4), 329-335.

Shen, K., Sun, H. L., Ji, G., Yang, Y., Jiang, Z., & Song, F. (2016). Fabrication and characterization of organic–inorganic hybrid perovskite devices with external doping. *Nanoelectronics and Materials Development*, 95.

Slami, A., Bouchaour, M., & Merad, L. (2020). Comparative study of modelling of Perovskite solar cell with different HTM layers. *Int. J. Mater*, *7*, 2313-10555.

Stamate, M. D. (2003). On the dielectric properties of dc magnetron TiO_2 thin films. *Applied Surface Science*, *218*(1-4), 318-323.

Stanic, D., Kojic, V., Cizmar, T., Juraic, K., Bagladi, L., Mangalam, J., Rath, T., & Gajovic, A. (2021). Simulating the Performance of a Formamidinium Based Mixed Cation Lead Halide Perovskite Solar Cell. *Materials (Basel)*, *14*(21). https://doi.org/10.3390/ma14216341

Suhaimy, S. H. M., Ghazali, N., Arith, F., & Fauzi, B. (2020). Enhanced simazine herbicide degradation by optimized fluoride concentrations in TiO_2 nanotubes growth. *Optik*, *212*, 164651.

Tseng, Z.-L., Chiang, C.-H., Chang, S.-H., & Wu, C.-G. (2016). Surface engineering of ZnO electron transporting layer via Al doping for high efficiency planar perovskite solar cells. *Nano Energy*, *28*, 311-318.

Vogt, M., Tobon, C. R., Alcaniz, A., Procel, P., Blom, Y., El Din, A. N., Stark, T., Wang, Z., Goma, E. G., & Etxebarria, J. (2022). Introducing a comprehensive physics-based modelling framework for tandem and other PV systems. *Solar Energy Materials and Solar Cells*, *247*, 111944.